

Modeling exchange bias microscopically

U. Nowak, A. Misra and K. D. Usadel
 Theoretische Physik, Gerhard-Mercator-Universität Duisburg,
 47048 Duisburg, Germany
 e-mail: uli@thp.uni-duisburg.de

September 4, 2018

Abstract

Exchange bias is a horizontal shift of the hysteresis loop observed for a ferromagnetic layer in contact with an antiferromagnetic layer. Since exchange bias is related to the spin structure of the antiferromagnet, for its fundamental understanding a detailed knowledge of the physics of the antiferromagnetic layer is inevitable. A model is investigated where domains are formed in the volume of the AFM stabilized by dilution. These domains become frozen during the initial cooling procedure carrying a remanent net magnetization which causes and controls exchange bias. Varying the anisotropy of the antiferromagnet we find a nontrivial dependence of the exchange bias on the anisotropy of the antiferromagnet.

Keywords: Exchange biasing, magnetic multilayers, Heisenberg model, numerical simulations

1 Introduction

When a ferromagnet (FM) is in contact with an antiferromagnet (AFM) a shift of the hysteresis loop along the magnetic field axis can occur which is called exchange bias (EB). Usually, this shift is observed after cooling the entire system in an external magnetic field below the Néel temperature T_N of the AFM. Although this effect is well known since many years [1] and is already intensively exploited in magnetic devices its microscopic origin is still under debate. For a review of the experimental work see the recent article by Nogués and Schuller [2].

In the approach of Malozemoff [3] exchange bias is attributed to the formation of domain walls in the AFM perpendicular to the FM/AFM interface due to interface roughness. However, the formation of domains in the AFM only due to interface roughness is unlikely to occur because the creation of the domain walls is energetically unfavorable.

Koon considered a spin-flop coupling between FM and the compensated AFM as responsible for EB [4], but recently, Schultheiss and Butler [5, 6] showed that spin-flop coupling alone cannot account for this effect. Instead, in their model EB is only obtained if uncompensated AFM spins are assumed at the interface — their occurrence is not explained microscopically.

In a previous Letter Miltényi et al. [7] showed that it is possible to strongly influence EB in Co/CoO bilayers by diluting the antiferromagnetic CoO layer, i. e. by inserting non-magnetic substitutions ($\text{Co}_{1-x}\text{Mg}_x\text{O}$) or defects (Co_{1-y}O) not at the FM/AFM interface, but rather throughout the volume part of the AFM. In these systems the observed EB is primarily not due to disorder or defects at the interface. Rather, the full antiferromagnetic layer must be involved and it was argued that in these systems EB has its origin in a domain state in the volume part of the AFM which triggers the spin arrangement and the FM/AFM exchange interaction at the interface. This domain state develops due to the dilution of the AFM: the domain walls pass preferentially through non-magnetic sites thus reducing considerably the energy necessary to create a wall. The domain state strongly depends on the dilution of

the AFM resulting in a strong dependence of EB on dilution. Since dilution favors the formation of domains it leads to an increase of the magnetization in the AF and thus to a strong increase of the EB upon dilution (see also [8], where it was shown that it is possible to influence (to increase or even to reverse) EB by a subsequent ion irradiation of the sample).

In the same letter this picture was further supported by Monte Carlo simulations. Later it was shown [9, 10] that a variety of experimental facts associated with exchange bias can be explained within our model, like positive exchange bias after cooling in strong magnetic fields, the temperature dependence of exchange bias, especially the relation between the so-called blocking temperature and the Néel temperature, and the training effect, among others. In these studies the AFM CoO investigated experimentally was due to its rather strong uniaxial anisotropy modeled as Ising system which is from a numerical point of view an ideal candidate to study basic properties of EB. However, since the occurrence of EB is not restricted to systems with a strong anisotropy in the AFM, in the present paper we will extend the previous model [7, 9, 10] to the non-Ising case, i. e. we will vary the strength of the anisotropy of the AFM.

In the next section we give a brief review of the physics of domains in diluted Ising antiferromagnets in an external field. These systems have been studied in great detail in the past and the physics which emerge from these studies are important for understanding EB. In Sec. 3 our model is described and in Sec. 4 our results from Monte Carlo simulations are discussed. Finally, we summarize in the last section.

2 Domains in disordered antiferromagnets

Considerable interest has been focused in recent years on the understanding of diluted Ising antiferromagnets in an external magnetic field (DAFF) as they are ideal candidates for the study of disordered systems. A typical material for experimental studies is $\text{Fe}_{1-p}\text{Zn}_p\text{F}_2$ where FeF_2 is

the AFM which is randomly diluted with probability p by non-magnetic Zn ions. Theoretically, due to the very strong uniaxial anisotropy this system is usually treated as Ising model. Properties which have been extensively exploited are the critical behavior, domain structures, metastability and slow dynamics (for reviews on DAFF see [11, 12]). Additionally, many of the findings of the DAFF are also relevant for the random field Ising model (RFIM) which has been shown to be in the same universality class [13, 14].

In zero field the system undergoes a phase transition from the paramagnetic phase to the long-range ordered, antiferromagnetic phase at the disorder dependent Néel temperature T_N as long as the dilution p is small enough so that the lattice of occupied sites is above the percolation threshold. In the low temperature region, for small magnetic fields B the long-range ordered phase remains stable in three dimensions [15, 16], while for higher fields the DAFF develops a disordered domain state [17, 18] with a spin-glass-like behavior. The reason for the domain formation was originally investigated by Imry and Ma for the RFIM [19]. The driving force for the domain formation is a statistical imbalance of the number of impurities of the two antiferromagnetic sublattices within a finite region of the DAFF. This leads to a net magnetization of this region which couples to the external field. A spin reversal of this region, i. e. the creation of a domain can hence lower the energy of the system. The necessary energy increase due to the formation of a domain wall can be minimized if the domain wall passes preferentially through non-magnetic defects at a minimum cost of exchange energy. Hence, these domains have non-trivial shapes following from an energy optimization. They have been shown to have a fractal structure with a broad distribution of domain sizes and with scaling laws quantitatively deviating from the original Imry-Ma assumptions [20, 21].

In small fields the equilibrium phase of the three-dimensional DAFF is long-range ordered. However, if cooled in a field B below a certain temperature $T_i(B)$, the system usually also develops metastable domains [22, 23]. The reason for this metastability is a strong pinning which hin-

ders domain wall motion. These pinning effects are due to the dilution (random-bond pinning) as well as due to the fact that a rough domain wall also carries magnetization in a DAFF (following again the Imry-Ma argument) which couples to the external field and hinders domain wall motion (random-field pinning) [24]. Consequently, after cooling the system from the paramagnetic phase within an external field, a DAFF freezes in a metastable domain state which survives even after switching off the field, then leading to a remanent magnetization which decays extremely slow [25].

In the following we will argue that these well established properties of the DAFF are the key for understanding exchange bias. Indeed, during preparation of the system, the AFM is cooled in an external magnetic field and additionally under the influence of an effective interface exchange field stemming from the magnetized FM. Hence, the AFM — as far as it is diluted in any sense — must develop a domain state with a surplus magnetization similar to that of a DAFF after field cooling.

3 Model for exchange bias

The model which we consider in the following consists of one FM monolayer exchange coupled to a diluted AFM film consisting of t monolayers. In Fig. 1 a sketch of our model is shown for $t = 3$.

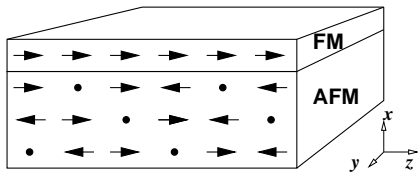


Figure 1: Sketch of the model with one FM layer and three diluted AFM layers. The dots mark defects (non-magnetic ions).

The system is described by a classical Heisenberg model,

$$\mathcal{H} = -J_{\text{FM}} \sum_{\langle i,j \rangle} \underline{S}_i \cdot \underline{S}_j - \sum_i (d_z S_{iz}^2 + d_x S_{ix}^2 + \underline{S}_i \cdot \underline{B})$$

$$\begin{aligned} & -J_{\text{AFM}} \sum_{\langle i,j \rangle} \epsilon_i \epsilon_j \underline{\sigma}_i \cdot \underline{\sigma}_j - \sum_i (k_z \epsilon_i \sigma_{iz}^2 + \epsilon_i \underline{\sigma}_i \cdot \underline{B}) \\ & -J_{\text{INT}} \sum_{\langle i,j \rangle} \epsilon_i \underline{\sigma}_i \cdot \underline{S}_j, \end{aligned}$$

where the first line contains the energy contributions of the FM. Here, the first term is the ferromagnetic nearest neighbor interaction with exchange constant J_{FM} . The second term introduces an easy axis in the FM (z -axis, anisotropy constant $d_z = 0.1 J_{\text{FM}}$) which sets the Stoner-Wohlfarth limit of the coercive field, i. e. the zero temperature limit for magnetization reversal by coherent rotation ($B_c = 2d_z$, in our units, for a field parallel to the easy axis). The shape anisotropy is approximated by the next term (anisotropy constant $d_x = -0.1 J_{\text{FM}}$) leading to a magnetization which is preferentially in the $y-z$ -plane. We checked, however, that its value does not influence our results. The last term of the first line is the Zeemann energy.

The second line describes the diluted AFM ($\epsilon_i = 0, 1$; dilution p) correspondingly except of the shape anisotropy. For the exchange constant of the AFM which mainly determines its Néel temperature (also depending on the dilution and the uniaxial anisotropy k_z) we set $J_{\text{AFM}} = -J_{\text{FM}}/2$. Finally, the third line includes the interface coupling between FM and AFM and for simplicity we assume $J_{\text{INT}} = -J_{\text{AFM}}$.

Our magnetic field B will always be along the z axis. In earlier publications [7, 9, 10] the AFM was described by an Ising model. In the present work, we relax this restriction on the AFM. In order to investigate a broader class of systems for the AFM we vary the uniaxial anisotropy k_z of the AFM.

4 Results from Simulations

We use Monte Carlo methods with a heat-bath algorithm and single-spin flip methods for the simulation of the model explained above. Each spin is subject to a trial step consisting of a small deviation from the original direction followed by a second trial step in form of a total flip. This two-fold trial step can take care of a broad range of anisotropies starting from very soft spins up to the Ising limit [26]. We perform typically 25000

Monte Carlo steps per spin for a complete hysteresis loop.

Since we are not interested in the critical behavior of the model above, we do not perform a systematic finite-size analysis. However, in order to observe the domain structure of the AFM we have to guarantee that typical length scales of the domain structure fit into our system. Therefore, we show here only results for rather large systems of lateral extension 128×128 . Nevertheless, we also varied the system size and checked that our results are not influenced by the system size as long as the system is not much smaller.

In our simulations the system is cooled from above to below the ordering temperature of the AFM. During cooling the FM is long-range ordered along the easy z axis and its magnetization is practically constant, resulting in a nearly constant exchange field for the AFM monolayer at the interface. In addition to this exchange field the external, magnetic field acts also on the whole AFM.

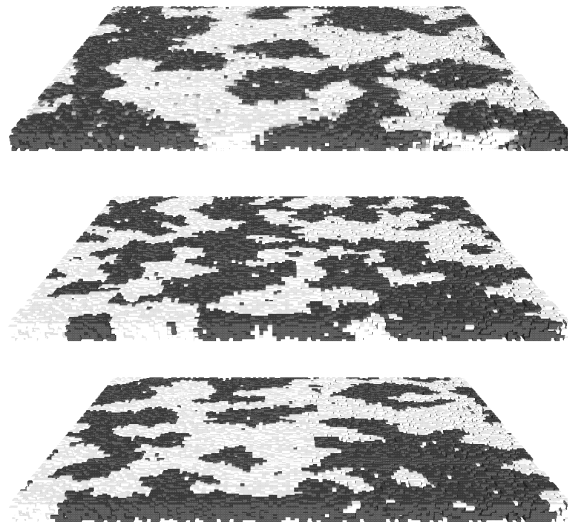


Figure 2: Frozen domain states of a 40% diluted AFM consisting of 6 monolayers for different values of the AFM anisotropy, $k_z = 0.1 J_{\text{FM}}, 1.0 J_{\text{FM}}, 30 J_{\text{FM}}$ (from top). The shading codes the z -component of the staggered magnetization.

As already argued in the section before, during the cooling procedure the AFM becomes frozen in a domain state, the structure of which depends on the system parameters. The influence on dilution [10] and the influence of the AFM film thickness [9] was already discussed before for the case of an Ising AFM. In the present case, typical staggered domain configurations of the bulk AFM are shown for three different values of the AFM anisotropy (Fig. 2). For low anisotropies $k_z < J_{\text{AFM}}$ domain walls have a width of the order of $\sqrt{J_{\text{AFM}}/k_z}$. Even for the lowest anisotropy shown in Fig. 2 the width is only of the order of a few lattice constants which can hardly be detected in our figure. Also, due to the dilution walls tend to follow the holes so that the wall width is further reduced at those places. Interestingly, the domain structure itself depends also on k_z . The system has the smallest domains for an intermediate value of $k_z = J_{\text{FM}}$ and not for the Ising case corresponding to the high anisotropy limit $k_z = 30 J_{\text{FM}}$ as one might expect. We will discuss the results following from this behavior later in connection with the anisotropy dependence of the EB.

Typical hysteresis loops taken after cooling in a field of $B = 0.25 J_{\text{FM}}$ are depicted in Fig. 3. Shown are results for the magnetization of the FM (upper figure) as well as that of the AFM interface layer (lower figure). An exchange bias is observed clearly and we determine the corresponding exchange bias field as $B_{\text{EB}} = (B^+ + B^-)/2$ where B^+ and B^- are those fields of the hysteresis loop branches for increasing and decreasing field, where the easy axis component of the magnetization of the FM becomes zero.

The interface magnetization of the AFM also shows a hysteresis, following the coupling to the FM. Additionally, its curve is shifted upwards due to the fact that after field cooling the AFM is in a domain state with a surplus magnetization. The upward shift of the hysteresis loop for the interface AFM proves the existence of remanent magnetization in the AFM domains. This shifted interface magnetization of the AFM acts as an additional effective field on the FM, resulting in EB. The magnitude of the EB field strongly depends on the amount of this upward shift. Note that the shift is of the order of a few percent of the satu-

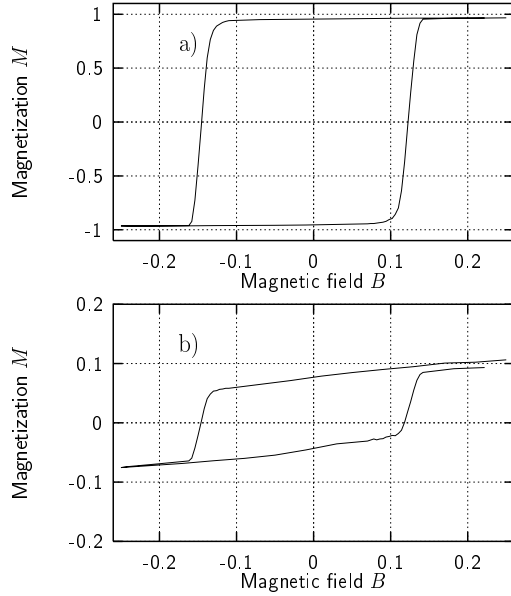


Figure 3: Typical hysteresis loop along z of a) the FM and b) the interface layer of the AFM, for a dilution $p = 0.4$ and an AFM thickness $t = 2$. The magnetization is in units of the saturation value and the field in units of J_{FM} .

ration magnetization of the AFM while approximately 10% of the spins of the AFM contribute to the AFM hysteresis. The saturation field for the AFM is much larger than that of the FM so that the AFM is never saturated during the simulation.

In absence of any anisotropy in the FM and at very low dilution of the AFM we observe a perpendicular coupling between FM and AFM. The magnetization reversal in the FM is here by coherent rotation. The picture changes with increasing uniaxial anisotropy in the FM and upon further dilution of the AFM. The magnetization reversal in the FM is now by domain wall motion and the perpendicular coupling becomes less significant. This is because uniaxial anisotropies in both the FM and the AFM having the same axis no longer lead to an energy minimum for a perpendicular coupling across the interface. Moreover AFM spins with missing AFM neighbors can lower their energy by rotating parallel to their FM neighbors. Therefore, in the framework of our calculations a spin-flop coupling is not an essential mechanism

for EB.

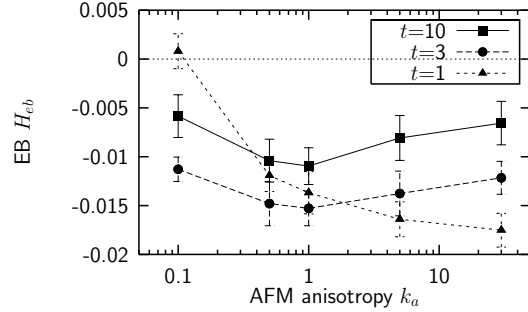


Figure 4: EB field versus anisotropy of the AFM for different AFM thicknesses (numbers of AFM layers). Field and anisotropy are in units of J_{FM} .

We have calculated the EB field for a wide range of values of k_z , starting from very soft spins to rigid, Ising-like spins. Fig. 4 shows result for different thicknesses of the AFM and for a dilution of $p = 0.4$. Interestingly, we find a peak in the EB field at an intermediate value of k_z for a sufficiently thick AFM while at lower thicknesses the EB field increases with the anisotropy and saturates in the Ising limit.

The key for the understanding of EB is the understanding of AFM domain configurations and domain walls. AFM domains are required to carry a surplus magnetization at the interface which must be stable along the z direction during hysteresis in order to produce any EB. In general, one might expect that the most stable domain configurations are obtained for the Ising limit. But Fig. 4 and also Fig. 2 suggest that the behavior of domains is more complex. Let us start considering the Ising limit where some domain wall is formed upon field cooling. This domain wall preferentially passes through defects thereby minimizing the exchange energy and at the same time it gathers magnetization thereby lowering the Zeeman energy. When the anisotropy k_z is decreased the energy to create a domain wall will decrease. Thus the system will respond by roughening the domain boundaries (see Fig. 2, where the domain configuration in the middle is more complex than the lower one which represents the Ising limit). This roughening enhances the possi-

bility for the domains to carry any surplus magnetization and hence the EB will increase. However, there exists a counter effect. While further decreasing k_z the width of the domain wall increases, so that less energy can be saved through the dilution. Hence, for still lower anisotropy the domain walls will smoothen thereby lowering again the exchange energy (see once again Fig. 2, now comparing the domain configuration in the middle with the upper one for still lower anisotropy which has much smoother domain walls). Since flat walls carry less remanent magnetization the EB will decrease now with decreasing anisotropy. The compromise between these two opposite effects is achieved at some intermediate value of k_z where the bias shows a peak.

However, the peak disappears at lower values of t . This happens since for only one monolayer of AFM we are close to the percolation threshold where the domain walls pass nearly exclusively through the defects costing very little or no energy. Therefore the first mechanism discussed above is less important and the EB increases with k_z till it saturates in the Ising limit.

5 Conclusions

In conclusion, we find that the domain state model for EB proposed originally for the Ising AFM is not restricted to this limit. Rather under certain combination of thickness and dilution of the AFM, the softness of the AFM spins can lead to an even stronger bias field. Since disorder in the AFM of an exchange bias system is rather common, our model yields a general understanding of the microscopic origin of exchange bias. Within our model there are several properties which influence the bias field, such as dilution, thickness and anisotropy of the AFM. Although a qualitative understanding regarding the dependence of EB on these parameters has been achieved, a quantitative study of the domain structure both at the interface and in the bulk of the AFM would provide a deeper understanding to the problem.

Acknowledgments

This work has been supported by the Deutsche Forschungsgemeinschaft through SFB 491 and Graduiertenkolleg 277.

References

- [1] W. H. Meiklejohn and C. P. Bean, Phys. Rev. **102**, 1413 (1956).
- [2] J. Nogu  s and I. K. Schuller, J. Magn. Magn. Mat. **192**, 203 (1999).
- [3] A. P. Malozemoff, Phys. Rev. B **35**, 3679 (1987).
- [4] N. C. Koon, Phys. Rev. Lett. **78**, 4516 (1998).
- [5] T. C. Schulthess and W. H. Butler, Phys. Rev. Lett. **81**, 4516 (1998).
- [6] T. C. Schulthess and W. H. Butler, J. Appl. Phys. **85**, 5510 (1999).
- [7] P. Milt  nyi, M. Gierlings, J. Keller, B. Beschoten, G. G  ntherodt, U. Nowak, and K. D. Usadel, Phys. Rev. Lett. **84**, 4224 (2000).
- [8] A. Mougin, T. Mewes, M. Jung, D. Engel, A. Ehresmann, H. Schmoranz, J. Fassbender, and B. Hillebrands, Phys. Rev. B **63**, 60409 (2001).
- [9] U. Nowak, A. Misra, and K. D. Usadel, J. Appl. Phys. **89**, 7269 (2001).
- [10] U. Nowak and K. D. Usadel, Phys. Rev. B (2001), in preparation.
- [11] W. Kleemann, Int. J. Mod. Phys. B **7**, 2469 (1993).
- [12] D. P. Belanger, in *Spin Glasses and Random Fields*, edited by A. P. Young (World Scientific, Singapore, 1998).
- [13] S. Fishman and A. Aharony, J. Phys. C **12**, L729 (1979).
- [14] J. L. Cardy, Phys. Rev. B **29**, 505 (1984).

- [15] J. Z. Imbrie, Phys. Rev. Lett. **53**, 1747 (1984).
- [16] J. Bricmont and A. Kupiainen, Phys. Rev. Lett. **59**, 1829 (1987).
- [17] F. C. Montenegro, A. R. King, V. Jaccarino, S.-J. Han, and D. P. Belanger, Phys. Rev. B **44**, 2255 (1991).
- [18] U. Nowak and K. D. Usadel, Phys. Rev. B **44**, 7426 (1991).
- [19] Y. Imry and S. Ma, Phys. Rev. Lett. **35**, 1399 (1975).
- [20] U. Nowak and K. D. Usadel, Phys. Rev. B **46**, 8329 (1992).
- [21] J. Esser, U. Nowak, and K. D. Usadel, Phys. Rev. B **55**, 5866 (1997).
- [22] R. J. Birgeneau, R. A. Cowley, G. Shirane, and H. Yoshizawa, J. Stat. Phys. **34**, 817 (1984).
- [23] D. P. Belanger, M. Rezende, A. R. King, and V. Jaccarino, J. Appl. Phys. **57**, 3294 (1985).
- [24] J. Villain, Phys. Rev. Lett. **52**, 1543 (1984).
- [25] S.-J. Han, D. P. Belanger, W. Kleemann, and U. Nowak, Phys. Rev. B **45**, 9728 (1992).
- [26] U. Nowak, in *Annual Reviews of Computational Physics IX*, edited by D. Stauffer (World Scientific, Singapore, 2000), p. 105.